

Cite this article as: Chen Yang, Hu Jichong, Huang Hailiang. Effects of Composition and Environment on Oxidation Behavior of Nickel-Based Superalloys[J]. Rare Metal Materials and Engineering, 2024, 53(07): 1897-1908. DOI: 10.12442/j.issn.1002-185X.20230649.

REVIEW

Effects of Composition and Environment on Oxidation Behavior of Nickel-Based Superalloys

Chen Yang, Hu Jichong, Huang Hailiang

Institute for Advanced Studies in Precision Materials, Yantai University, Yantai 264005, China

Abstract: Ni-based superalloys exhibit exceptional mechanical properties and high-temperature resistance, making them suitable for use in aggressive environments. The oxidation behavior of Ni-based superalloys is primarily influenced by the intrinsic material properties and oxide scale properties, which are largely dependent on the complex composition and content of alloying elements. Various environmental parameters, including atmosphere composition, temperature, stress and molten salts, directly impact the oxidation behavior of materials. The effects of alloying elements and the service environment on the oxidation behavior of Ni-based superalloys were comprehensively reviewed. Aluminium, chromium and cobalt are considered as favorable elements to form compact and adherent scales that protect the matrix. The addition of titanium, molybdenum, niobium, tungsten and tantalum is traditionally believed to be detrimental. However, recent researches have presented different opinions, which were discussed. The oxidation mechanism was also explored and an insight into the future developments of Ni-based superalloys was provided.

Key words: oxidation behavior; nickel-based; superalloy; alloying element; service environment

Ni-based superalloys possess excellent high temperature mechanical properties, including strength, toughness and creep resistance. Consequently, they are extensively utilized in the hottest parts of aircraft engines, gas turbines and chemical industries. However, these alloys are often exposed to harsh environments that require them to withstand higher temperatures, more complex stress conditions and more severe erosion^[1]. Oxidation can lead to material degradation or even premature failure due to the consumption of solutes and dissolution of strengthening phases from the oxide-affected zone, resulting in significant economic losses^[2]. Therefore, it is imperative to study and to understand the oxidation behavior and mechanisms of these superalloys in order to mitigate or prevent oxidation-related losses and extend their service life.

The oxidation behavior of Ni-based superalloys is highly dependent on intrinsic material properties such as chemical composition and microstructure, as well as service environments including oxidation temperature, oxidation atmosphere, self-generated stress and external load. Additionally, the properties of the oxide scale, such as thermo-

stability, mechanical properties and phase structure, also play a crucial role^[3-5]. This research primarily reviewed the effects of alloying elements and service environment on the oxidation behavior of Ni-based superalloys. It has been proven that the addition of even minor alloying elements (<10at%) and trace elements (<1at%) will induce considerable impact on the formation of oxide products and greatly influence the oxidation properties of the superalloys^[6]. The chemical composition of superalloys is extremely complex, and the differences in phase composition and microstructure lead to different oxidation mechanisms during the oxidation process. Moreover, the chemical composition of superalloys also affects the intrinsic properties of the oxide scale, which in turn determines whether the film can effectively protect the matrix. Therefore, understanding the effects of various alloying elements on the oxidation resistance of Ni-based superalloys is crucial for optimizing existing materials and developing new ones.

Various environmental parameters are fundamental factors that directly affect the oxidation behavior of materials. The composition of the atmosphere, which may contain hydrogen,

Received date: October 17, 2023

Foundation item: National Key R&D Program of China (2021YFB3700401); Shandong Provincial Natural Science Foundation for Youths (ZR2022QE234)

Corresponding author: Chen Yang, Ph. D., Lab Master, Institute for Advanced Studies in Precision Materials, Yantai University, Yantai 264005, P. R. China, E-mail: chenyang@ytu.edu.cn

Copyright © 2024, Northwest Institute for Nonferrous Metal Research. Published by Science Press. All rights reserved.

sulfur, steam or other impurities, can significantly influence the oxidation behavior depending on the concentration and combination of gases^[7-8]. Additionally, environmental parameters such as temperature (isothermal oxidation or cyclic oxidation), atmosphere pressure, stress applied to samples and the presence of molten salts also play important roles^[9-10]. In practical oxidation process, multiple factors may be activated simultaneously, or one specific factor may dominate. Therefore, it is necessary to assess and to analyze the oxidation behavior in terms of the specific material and service environment.

1 Effects of Alloying Elements on Oxidation Behavior

The addition of alloying elements has a significant impact on the phase structure and microstructure of both the matrix and oxide scales, thereby influencing the oxidation behavior of superalloy. Typically, more than eight alloying elements are added to obtain the desired hardening effect, making it difficult to analyze the individual effect of each alloying element on oxidation behavior^[11]. In fact, some oxide products have a lower melting point than the pure metal itself, causing them to melt under service conditions and lose their protective function. Table 1 lists several oxides, sulfides and chlorides with low melting point.

1.1 Aluminium, chromium and silicon

The microstructure of Ni-based superalloys usually consists of a solid solution matrix phase γ (Ni) and nearly 70vol% cuboidal reinforcement phase γ' (Ni_3Al), which both exhibit

relatively good oxidation resistance. However, deleterious phase such as δ (Ni_3Nb) and η (Ni_3Ti) may sometimes appear^[12]. In general, the formation of continuous, compact and adherent Al_2O_3 , Cr_2O_3 and SiO_2 oxides promises good oxidation resistance. Cr_2O_3 oxide scales act as a protective barrier below 871 °C, while the Al_2O_3 oxide scale plays a role in protecting the matrix above 1000 °C due to the rapid volatilization of Cr_2O_3 . The Al_2O_3 phase possesses a stable corundum structure, low Gibbs free energy and low Pilling-Bedworth ratio (1.28). The oxidation resistance of γ , γ' and β is improved with increasing the Al content. Wollgarten et al^[4] proved that the addition of 3wt% Al in Ni-14Cr-9Co (wt%) alloys stabilizes the Cr_2O_3 scale and significantly restrains the formation of dispersed Ni-oxides when oxidized at 950 °C for up to 100 h.

A protective Cr_2O_3 scale tends to form when the Cr concentration surpasses 10wt% at temperatures below 1000 °C^[11]. The addition of above 5at% Al contributes to the formation of passive chromia. In Ni-5Cr and Ni-15Cr alloys, $\text{Cr(III)}_2\text{O}_3$ oxide islands usually form in the initial oxidation stage, which are then covered by Ni(II)O immediately. However, in Ni-30Cr and ternary alloys, chromia rapidly grows and NiO hardly remains. It has been reported that transient NiO and $\text{Ni(Cr, Al)}_2\text{O}_4$ spinel may form on Ni-Cr-Al based superalloys (with approximately 20wt% Cr) in the early stages of oxidation^[12]. However, these transient oxides are rarely detected with prolonging the oxidation time.

The mechanism of the beneficial effect of silicon (Si) is controversial for decades. Wang et al^[13] fabricated Ni-15Cr-

Table 1 Different oxides, sulfides and chlorides with low melting point^[3]

Metal	Melting point/°C	Oxide	Oxide melting point/°C	Sulfide	Sulfide melting point/°C	Chloride	Chloride melting point/°C
Boron	2200	B_2O_3	460				
Antimony	630.7	Sb_2O_3	656				
Cadmium	321.2	CdO	700				
Bismuth	271.4	Bi_2O_3	824				
Plumbum	327.4	PbO	888				
Vanadium	1750	V_2O_5	690				
Molybdenum	2610	MoO_2	777	MoS_2	>1800	MoCl_5	194
		MoO_3	795				
		WO_2	1277				
Tungsten	3410	WO_2	1277	WS_2	>1800	WCl_6	240
		WO_3	1473				
Chromium	1875					CrCl_3	820
Iron	1538			FeS_2	742	FeCl_2	676
				Ni_3S_2	806	FeCl_3	303
				Ni_7S_6	573		
Nickel	1453	NiO	1990	NiS	992	NiCl_2	1030
				Ni_3S_4	356		
Aluminium	660.4	Al_2O_3	2015	Al_2S	960	AlCl_3	193
Silicon	1410	SiO_2	1713	SiS_2	1090	SiCl_4	-70

5Al- x Si ($x = 0, 1, 3, 5$, wt%) superalloys to study the effect of Si on cyclic oxidation behavior at 1100 °C. The results show that the addition of 3wt% Si facilitates the formation of continuous metastable alumina (θ -Al₂O₃ and γ -Al₂O₃) and stable alumina (α -Al₂O₃) scales, and contributes to the transformation of metastable alumina into stable alumina. At the same time, Si addition enhances the adhesion of the interface between the matrix and oxide scale. However, a higher Si content might cause stress in the scales and weaken the adhesion. Anzini et al^[14] assessed the oxidation, sulfidation and hot corrosion of three variant polycrystalline powder superalloys (baseline, 1wt% Mn and 0.5wt% Si) at 750 °C. The results demonstrated that the addition of 0.5wt% Si contributes to the formation of a protective and continuous Cr₂O₃-Al₂O₃ dual layer (as shown in Fig. 1). This addition also decreases the depth of sulfidation by 2/3 and the depth of hot corrosion by 1/2. It was also reported that Si tends to segregate at grain boundaries and may inhibit the inward diffusion of sulfur, thus enhancing the resistance to sulfidation^[15].

1.2 Titanium, cobalt, molybdenum and tungsten

It seems that the formation of TiO₂ and NiTiO₃ oxides cannot provide effective protection. However, Barth et al^[16] fabricated Ni-26Cr-10Al- x Ti ($x=0, 0.6, 1.7$) superalloys to explore the effect of Ti on oxidation in the early stages. The results proved that the Ti addition does not change the phase and thickness of the oxides, but it does accelerate the growth of Cr₂O₃ before the formation of a continuous Al₂O₃ layer. Wollgarten et al^[4] also demonstrated that the p-type Ti-doping (5wt%) in Ni-14Cr-9Co-3Al superalloy contributes to the growth of Cr₂O₃ scale while completely suppressing the formation of Ni-oxide. It might be attributed to the p-type Ti-doping of chromia, which accelerates the formation of Cr-ion vacancies, thereby enhancing the transport of cations through the scale.

Co has a solid solution strengthening effect on the

microstructure of superalloys. Pan et al^[17] investigated the effect of different Co contents (5.9wt%, 9.0wt% and 12.0wt%) on the solidification characteristics and microstructure of Ni-based single crystal (Ni-SC) superalloys. It was found that increasing the Co content can lower the precipitation temperature of the γ' phase and inhibit the dendritic segregation of Re, W and Cr elements. The addition of 9.0wt% Co results in the shortest primary dendrite arm spacing and the lowest ($\gamma + \gamma'$) eutectic content, achieving a more homogenized microstructure. Caldwell et al^[18] also claimed that Co addition reduces the segregation of Re in Ni-SCs without Ru. On the contrary, researches suggest that Co exacerbates the segregation of Re. Therefore, the effect of Co addition on the distribution of elements in Ni-SCs remains controversial. Bopape et al^[19] conducted a study on the impact of 30wt%–45wt% Co and 5wt%–20wt% Fe on the microstructure and corrosion behavior of heat-treated Ni-Fe-Co superalloys in 3.5wt% NaCl aqueous solution. The results indicated that the corrosion resistance of the alloys is improved with increasing the Co content and decreasing the Fe content. Therefore, Ni-5Fe-45Co (wt%) exhibits the best corrosion resistance in as-sintered and heat-treated conditions. Lu et al^[20] also demonstrated that Ni-Fe-based superalloys with high Co content possess excellent oxidation resistance. Additionally, the Co addition stimulates the formation of Cr₂O₃ oxide layer. Meng et al^[21] came to the same conclusion, stating that the partial replacement of W with Co in Ni-based superalloys promotes the formation of chromia scale. Moreover, the addition of Co inhibits the internal oxidation/nitridation of Al and enhances the adhesion of the scale. Furthermore, Co addition can improve the corrosion resistance of superalloys in molten Na₂SO₄-NaCl salts at 900 °C.

Mo and W elements are believed to be detrimental due to the rapid growth of non-protective oxides such as MoO₃, (MoWO)₃ and Ni(MoW)O₄, which impede the formation of

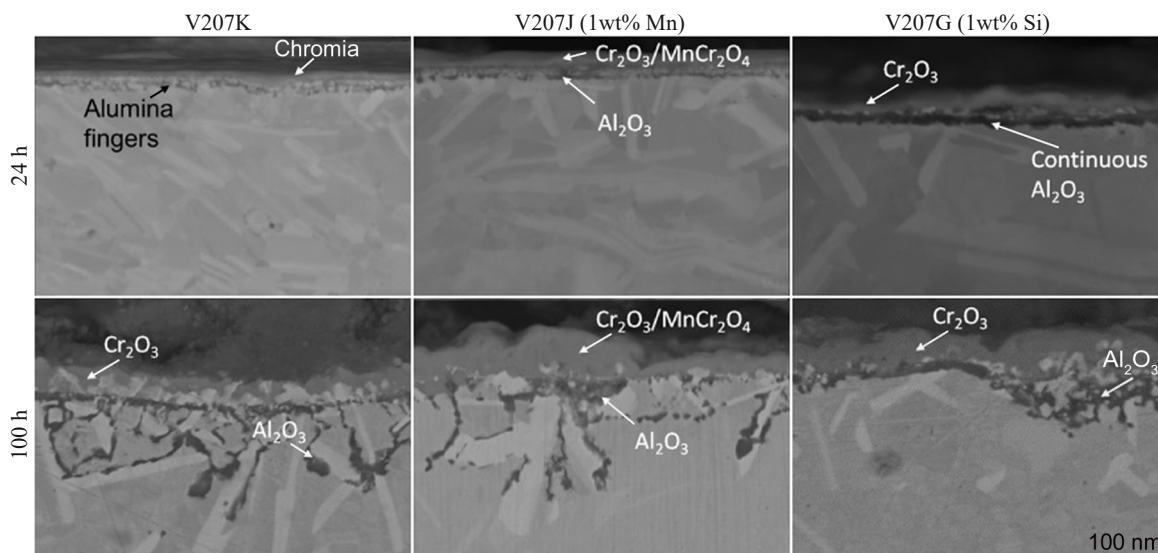


Fig. 1 BEI SEM micrographs of V207K, V207J and V207G alloys oxidized in air at 750 °C for 24 h and 100 h^[14]

the slowly-growing alumina scale^[22]. However, recent researches claim that Mo cations present in the Cr-rich oxide contribute to passivation and decrease in passivation breakdown. The oxidation mechanism of Mo and W elements in Ni-based superalloys is synergetic rather than singular^[23]. The existence of Mo and W creates favorable sites for oxygen chemisorption, stimulating the formation of MoO₂ and MoO₃ in the outer oxide layer. Mo and W may also be segregated at local corrosion sites, impacting local corrosion stabilization and repassivation, while inhibiting dissolution kinetics^[23].

Volders et al^[6] utilized near ambient pressure X-ray photoelectron spectroscopy (XPS) to investigate the impact of W on the initial steps of oxidation of Ni-5Cr, Ni-15Cr, Ni-30Cr and Ni-15Cr-6W at 500 °C and O₂ pressure of 10⁻⁴ Pa. The results show that the addition of W in Ni-15Cr-6W facilitates the reaction of Cr with oxygen, thus enhancing oxide quality. Fig. 2 shows a set of DFT calculations which display the most stable adsorption sites of O atoms in different Ni-based alloys.

1.3 Niobium, tantalum and hafnium

The presence of Nb is believed to have a highly detrimental effect on oxidation resistance^[22]. Ye et al^[1] found that a higher concentration of Nb in the novel powder metallurgy superalloy stimulates the partitioning of Al in the γ' phase. This slows down the outward diffusion of Al and facilitates the penetration of O into the alloy matrix, resulting in deeper internal oxidation. Fig. 3 shows the cross-section morphologies of the 0Nb, 0.5Nb, 1Nb and 2Nb alloys under BSE mode after oxidation at 1000 °C for 24, 72 and 100 h. In the Nb-free alloy, a continuous and compact Al₂O₃ layer forms between CrTaO₄ and the alloy matrix. However, as the Nb content increases, the Al₂O₃ tends to be finer and more dispersed. The presence of Nb leads to the formation of an Nb-containing Laves phase at the interface of the oxide scale and the matrix, which limits the diffusion of metallic cations and contributes to oxidation resistance. However, the Laves phase in the alloy matrix aggravates the diffusion of oxygen, causing detrimental internal oxidation. The Nb-bearing superalloy promotes the formation of a continuous and compact external oxide scale, effectively preventing the vaporization and spallation of Cr₂O₃, thus improving oxidation resistance. However, at the same time, internal oxidation is accelerated^[24].

Park et al^[25] investigated the effects of Al and Ta on the

oxidation resistance of Ni-8Cr-9.5Co-2.5Mo-6W-(4-5)Al-2Ti-(3-6)Ta-0.1C-0.01B (wt%) superalloys at 850 and 1000 °C through cyclic oxidation tests. The results show that Ta addition reduces the formation of the continuous Al₂O₃ layer at 850 °C. However, when the concentration exceeds 5wt% at 850 or 1000 °C, the oxidation resistance will be elevated. Wollgarten et al^[4] confirmed that the 5wt% Ta addition to Ni-14Cr-9Co-3Al promotes the formation of a thin alumina scale at 950 °C for up to 100 h. Guo et al^[26] declared that the Ta addition in β -NiAl inhibits the outward diffusion of Al, thereby impairing the growth of protective oxide scales. However, Han et al^[27] claimed that a (Cr, Ti)TaO₄ layer forms inside the corrosion scale, which delays the diffusion of elements and increases the hot corrosion resistance of the directionally solidified Ni-based superalloy in fused sodium sulphate (Na₂SO₄) at 900 °C. Yang et al^[28] also illustrated that incorporating within 5wt% Ta element results in the displacement of Cr, Ti and Al into the γ phase, and concurrently diminishes the solubility of oxygen in the γ solid solution. The formed Ta₂O₅ and (Ti/Cr)TaO₄ oxidation products are readily combined with Cr₂O₃ to generate CrTaO₄, which in turn impedes the volatilization of Cr₂O₃, thereby enhancing the alloy's oxidation resistance. In summary, the influence of Ta element on the oxidation of Ni-based superalloys is conditional and controversial.

Minor addition of Hf contributes to the integrity of the oxidation scales by reinforcing scale adhesion to the matrix and absorbing impurities, such as sulfur^[29]. Hou et al^[30] claimed that a high Hf content can strengthen the grain boundaries by forming dispersed HfC along them. The movement of dislocation is restrained and the grain boundaries are pinned, thereby greatly improving the creep resistance and hardness of superalloys at high temperatures. However, Rehman et al^[31] assessed the oxidation properties of Hf single-doped and Hf/Y co-doped Ni-based superalloys at 900, 1000 and 1100 °C for up to 300 h. At 900 and 1000 °C, the undoped alloy exhibits the best oxidation resistance, while the Hf-doped alloy shows better scale adhesion. Co-doped Hf/Y components in the alloy minimize internal oxidation and elevate oxide scale adhesion to the matrix.

1.4 Other elements

Anzini et al^[14] proved that the addition of 1wt% Mn can improve the oxidation resistance by generating MnCr₂O₄

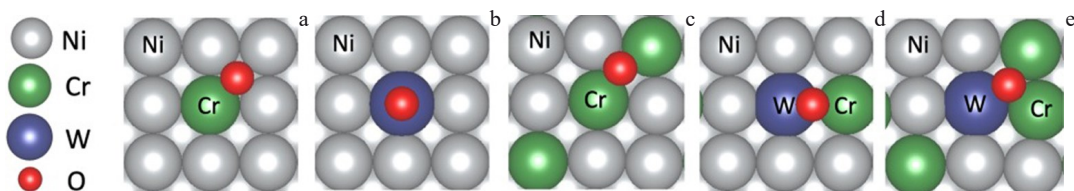


Fig.2 Summary of the most stable adsorption sites for atomic oxygen on different surfaces as calculated by DFT for fcc surfaces with one to four non-Ni atoms: (a) O binding energy= 3.81 V, at 1/9 Cr surface alloy and the lowest energy adsorption site is the Ni-Cr 4-fold site; (b) O binding energy=4.27 V, at 1/9 W surface alloy and the on-top O site is the most stable; (c) O binding energy=4.38 V, at 3/9 Cr surface alloy and the Cr-Ni-Cr hollow site is the most stable; (d) O binding energy=4.78 V, at 2/9 Cr/W surface alloy with the bridge site between W and Cr as the energetically favorable site; (e) O binding energy=5.00 V, at 4/9 Cr/W surface alloy and W-Cr-Cr hollow site is the most stable^[6]

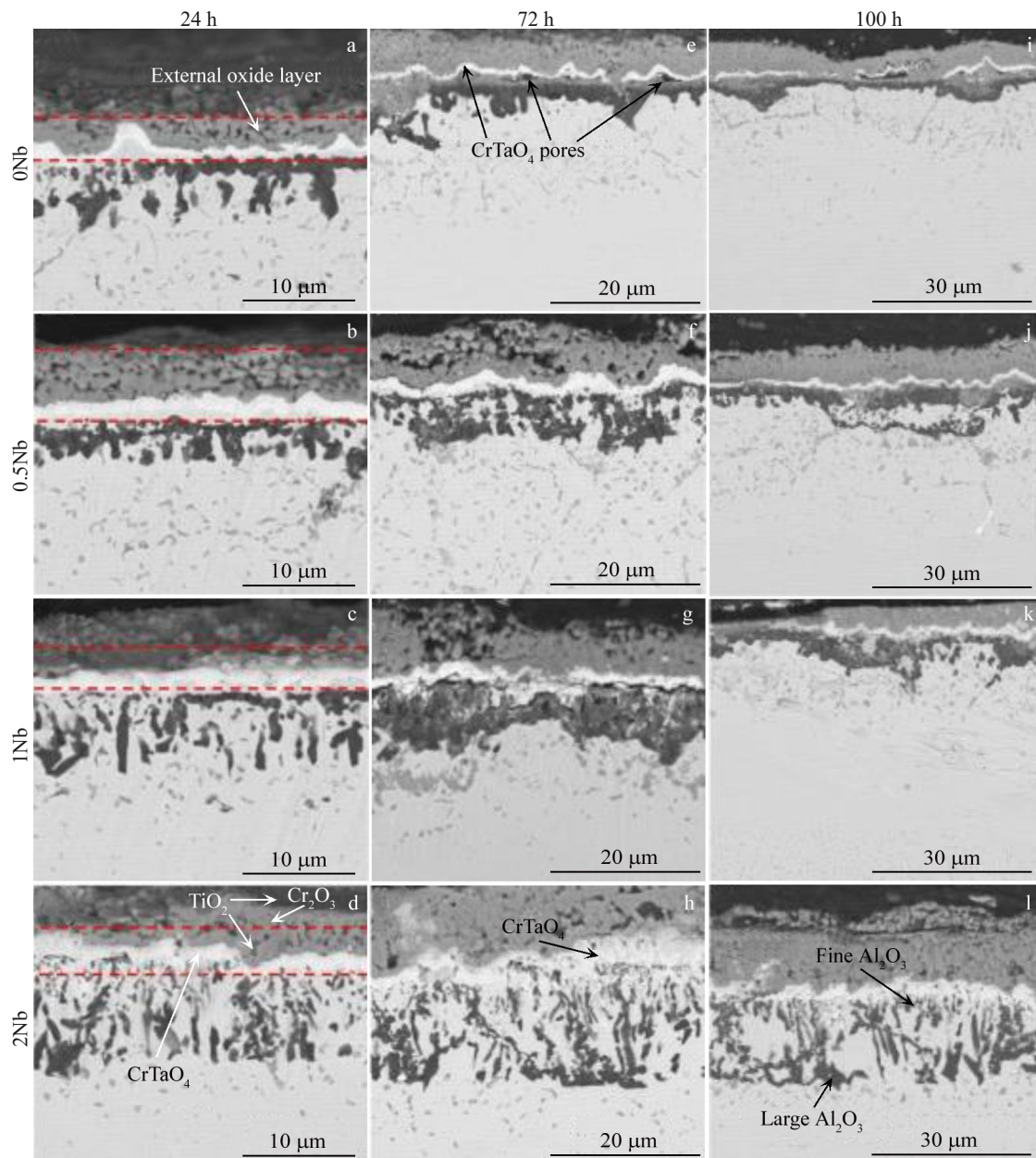


Fig.3 Cross-sectional morphologies of 0Nb, 0.5Nb, 1Nb and 2Nb alloys under BSE mode after oxidation at 101 325 Pa and 1000 °C for 24 h, 72 h and 100 h^[1]

instead of chromia after 24 and 100 h, while it cannot modify the alumina intrusion morphology. On the contrary, Mn decreases the oxidation resistance of Ni-Cr-W-Mo alloys, but its effect can be diminished by the addition of Al and Si^[32]. Pedrazzini et al^[33] illustrated that the oxide scale of a commercial Ni-based superalloy containing 1at% Mn presents a multi-phase layered structure. The atom probe tomography results showed that the phases are NiCr₂Mn₂O₄, a mix of Cr₂O₃ and spinel MnCr₂O₄ and rutile (Ti, Cr)O₂ from the uppermost to the interface, as shown in Fig.4. Additionally, the thickness of the Mn-containing alloy reduces by 3 times compared with that of the commercial Ni-based superalloy.

Li et al^[34] studied the effect of various Y concentrations (0.00, 0.05, 0.12, 0.21 and 0.43, wt%) on the oxidation

behavior of Ni-16Mo-7Cr-4Fe superalloy in air at 1273 K for 250 h. The results showed that the micro-addition of 0.05wt% Y cuts down the oxidation rate of the alloy by 30 times during steady-state stage. The addition of Y also stimulates the formation of a compact inner layer enriched with Cr₂O₃, remarkably improving the adhesion of the oxide scale.

Previous studies have reported that rare earth elements such as Dy, Hf, Zr and La can enhance the oxidation resistance of β-NiAl by single- or co-doping^[35]. Furthermore, the addition of Ru has been found to restrain the precipitation of the topologically close-packed phase, thereby increasing the microstructure stability of Ni-based single crystal superalloys^[36].

Research has proved that minor additions of reactive elements (REs) such as Y, Hf, Ce or their oxides (Y₂O₃, HfO₂,

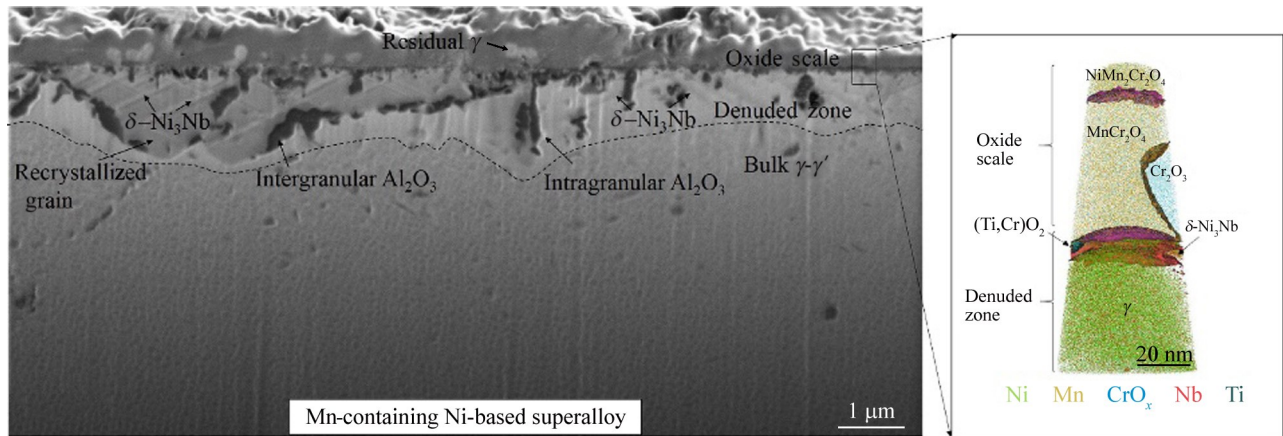


Fig.4 Focused ion beam micrograph showing the features and phases present in the oxide-affected zone (atom maps show different types of oxide, spinel and the δ phase in the denuded zone)^[33]

and CeO_2) help to enhance the adhesion of oxide scale^[37]. However, it has been observed that Ce has limited effectiveness at high temperatures, and the scale adhesion may even be weakened with increasing the oxidation time^[38]. Nevertheless, REs can effectively address unfavorable elements such as S, C and P, and annihilate vacancies to enhance the adhesion of the oxide scale^[38]. Liu et al^[39] studied the effect of trace amounts of RE on the oxidation resistance of Ni48-Cr28-W5-Co3-Mn1-Si1.6 superalloy. The results also illustrated that 0.20wt% RE addition has limited effect on oxidation resistance. During oxidation at 950–1150 °C for 100 h, a continuous layer of MnCr_2O_4 and Cr_2O_3 and a discontinuous layer of SiO_2 are formed from the outermost layer to the interface.

2 Service Environment

The service environments of superalloy components include temperature, oxidation atmosphere environment, pressure and stress in the surrounding environment, molten salts, etc.

2.1 Oxidation atmosphere environment

It is well known that the H in the atmosphere can highly damage the mechanical properties (ductility, fracture toughness, fatigue crack growth (FCG), etc) of the superalloy components, which is known as hydrogen embrittlement (HE)^[40–41]. However, Takakuwa et al^[7] put forward an interesting perspective suggesting that H can surprisingly retard the FCG of coarse-grained microstructure without the presence of the δ phase under low-stress states. This is attributed to the formation of intense crack closure by changing the crack path. This research presented the possibility of enhancing H-assisted FCG resistance in alloy 718 by optimizing the metallurgical methods. Ogawa et al^[40] studied the tensile properties of Ni-based superalloy 718, which was exposed to approximately 90 $\mu\text{g/g}$ hydrogen. The purpose of the study was to reveal the mechanisms of H-related embrittlement. Fig.5 shows the schematic illustration of the new H-assisted crack nucleation mechanism and possible reason for H-

agglomeration at the fracture initiation site. The cracks primarily nucleate along the annealing twin boundary (ATB) and crystallographic slip plane (SP).

Superalloy components used in exhaust gases may be susceptible to S contamination. The corrosive S element reacts with the metal matrix, forming sulfates that can significantly threaten the service life of the superalloy. Liu et al^[42] investigated the hot corrosion behavior of a polycrystalline Ni_3Al -based superalloy in sulfur-containing atmosphere at 900 °C. The results show that the main corrosion products in the interdendritic regions are $\text{Ni}_3\text{S}_2+\text{Al}_2\text{O}_3$, while in the dominant $\gamma'+\gamma$ dendrite regions, the corrosion products are $\text{Ni}_3\text{S}_2+\text{Cr}_3\text{S}_4$. Allo et al^[43] studied the influence of S (1–82 $\mu\text{g/g}$) and water vapor on the oxidation resistance of Manaurite XA14[®]. The results show that when the S concentration is below 30 $\mu\text{g/g}$, Al_2O_3 layer can effectively protect the matrix. However, when the S content exceeds 40 $\mu\text{g/g}$, the oxidation rate is largely increased, especially with the presence of steam.

Li et al^[8] studied the impact of different oxygen concentrations (10%, 21%, 30%) on the oxidation behavior of Ni-based single crystal superalloy at 1100 °C. The results exhibit that the fitted parabolic oxidation rate constants possess a linear relationship with the oxygen concentrations. As the oxidation time increases, Al_2O_3 oxides form on the sample surfaces at oxygen concentrations of 10% and 21%. However, at oxygen concentration of 30%, a typical three-layer structure consisting of (Ni, Co)O, spinel and Al_2O_3 phases forms from the outer to the inner layer. Higher oxygen concentrations not only accelerate the oxidation rate but also deteriorate the adhesion of the oxide layer to the matrix. Kai et al^[44] investigated the oxidation behavior of the $\text{Ni}_2\text{FeCoCrAl}_{0.5}$ high-entropy superalloy at 900 °C in O_2 -containing (1.0×10^5 – 10×10^5 Pa) environments. The results showed that as the oxygen pressure increases, the oxidation rate accelerates, resulting in the formation of a thickened α - Al_2O_3 layer exclusively on the surface. At oxygen pressure of 1.0×10^5 Pa, a mixture of α - Al_2O_3 , Cr_2O_3 and M -Cr spinel ($M=\text{Ni, Fe or Co}$) is formed, which is similar to the above phases formed under

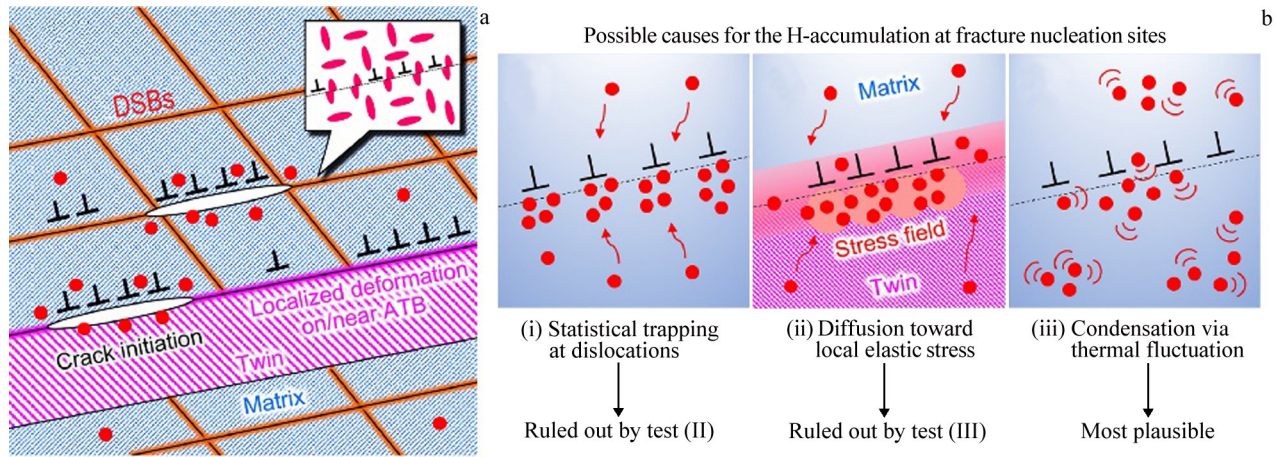


Fig.5 Schematic illustration of the new H-assisted crack nucleation mechanism along ATB and crystallographic SP owing to the reduced lattice cohesion via the accumulation of dislocations and hydrogen (a); possible rationales for H-agglomeration at the fracture initiation site (b)^[40]

30% oxygen atmosphere.

Superalloys are sometimes employed in steam environments, such as advanced ultra-supercritical (AUSC) boilers, which operate at very high pressures and temperatures. Consequently, these materials encounter numerous challenges, including creep rupture stem from wall thinning, increased rates of fire-side and steam-side corrosion and oxide spallation. Archana et al^[45] studied the oxidation characteristics of Ni-based superalloys 617 at 750 °C in ambient air and steam for up to 500 h. The samples exhibited more inferior oxidation resistance and adhesion under steam than ambient air. The primary phase in the external oxides of the samples in air is chromium, while the external oxide in the steam state contains detectable amounts of Al, Ti and H. Wu et al^[46] found that NiO and spinel oxides appear more rapidly in single crystal Ni-based superalloy in air with 15% H₂O than in dry air state at 900 °C. Wollgarten et al^[4] confirmed that the existence of 20vol% H₂O in the environment promotes the growth of Ni-rich oxides and leads to rapid breakaway oxidation in Al-free Ni-based alloys.

2.2 Temperature

The service temperatures of superalloys are still limited, so it is necessary to study how temperature influences oxidation behavior in order to develop new materials or upgrade existing superalloys. Xiao et al^[47] studied the oxidation behavior of a Ni-based superalloy with high Hf content (1.34wt%) oxidized at 900, 1000 and 1100 °C for 200 h. The alloy possesses excellent oxidation resistance, and no HfO₂ is observed in the oxide scale at 900 °C. However, as the temperature ascends to 1000 °C, HfO₂ particles form within the spinel phases of the scale, and peg-like HfO₂ is detected beneath the inner Al₂O₃ layer. The formation of peg-like HfO₂ is accelerated more rapidly (within 25 h) at 1100 °C. It can be deduced that Hf dissolves within the matrix and subsequently precipitates in situ, forming peg-like HfO₂ via diffusion. Wang et al^[48] investigated the oxidation behavior of GH738 in stagnant air at 800, 900 and 1000 °C, with exposure durations reaching up to 100 h. The results reveal that Cr₂O₃ is the predominant

external oxide at 800 °C, while TiO₂-Cr₂O₃ double-layer structure forms at 900 °C. The TiO₂ tends to diffuse to the outermost layer rather than the interface between the matrix and oxides. As the temperature rises up to 1000 °C, spallation emerges in the Cr_{0.12}Ti_{0.78}O_{1.74}Cr₂O₃ multi-layer oxide. Cao et al^[49] studied the microstructure evolution of Ni-based superalloy GH202 after oxidation from 800 °C to 1100 °C. The results show that as the temperature increases, the grains grow up, the big block carbides (MCs) decompose into carbon atoms which combine with Cr to form a few Cr-rich granular M₂₃C₆, and the hardness of the superalloy GH202 decreases. Li et al^[50] studied the high temperature oxidation resistance of Inconel 600 alloy exposed at 700, 800 and 900 °C for 100 h. The results demonstrated that the oxidation kinetic curves correspond to the parabolic dynamic rules (as shown in Fig.6) and the samples exhibit superior oxidation resistance at temperatures below 800 °C. The phases of Cr₂O₃ and NiCr₂O₄ form at 700 and 800 °C, and MnCr₂O₄ forms at 900 °C, which effectively protect the metal matrix from oxidation. However, the spallation easily occurs under applied force as the temperature surpasses 800 °C, due to the complicated component of the oxide film, which undermines adhesion.

2.3 Pressure and stress

Zhai et al^[51] elucidated the initial oxidation mechanism of a

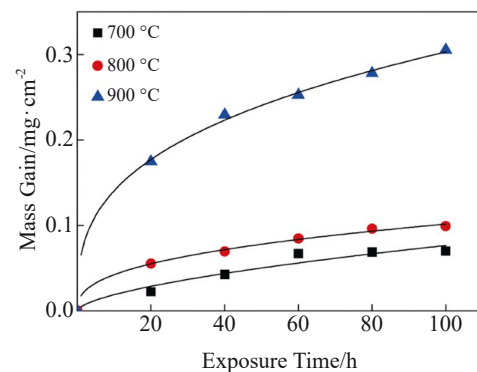


Fig.6 Oxidation kinetics curves of Inconel 600 alloy^[50]

Ni-based superalloy using a Cs-corrected environmental transmission electron microscope (ETEM). The impact of oxygen pressure (10^{-5} –10 Pa) on the initial oxidation behavior of the superalloy at 800 °C is shown in Fig.7. As the oxygen pressure increases to 10^{-1} Pa, the nanosized oxide particles start to nucleate preferentially at the interfaces of γ/γ' , as marked by the white arrow in Fig. 7c. When the pressure escalates to 10 Pa, cubic oxide particles start to nucleate within the γ' phase, as indicted by the yellow arrow in Fig. 7f. When the pressure arrives at 10 Pa, the particles gather to cover both the γ and γ' phases (Fig.7g).

Gu et al^[9] investigated the microstructure and corrosion characteristics of Hastelloy N under working stress in a molten salt environment. The results show that the corrosion products at the grain boundaries (GBs) are enriched in Cr, as shown in Fig. 8d, indicating that Cr diffusion deteriorates the integrity of the GBs, rendering them susceptible to corrosion crack invasion. Furthermore, stress accelerates Cr diffusion and GB carbide precipitation, thereby facilitating the

propagation of intergranular corrosion cracks into the grains by establishing a corrosion couple between the carbides and the matrix. Ramsay et al^[52] studied the oxidation behavior of the Ni-based superalloy RR1000 at 750 °C in air for 111 h under a peak elastic stress of 900 MPa. The results indicate that the stress minimally affects the thickness of the Cr_2O_3 layer, while it doubles the depth of the underlying intergranular Al_2O_3 layer compared to regions free of stress. This is attributed to the tensile stress at the Al_2O_3 intrusion site which increases the anion vacancy, thereby accelerating the Al_2O_3 growth rate. Consequently, the oxidation mechanism of Ni-based superalloys is not exclusive.

2.4 Hot corrosion in molten salts

Superalloys can be deployed in molten salt-based energy production, storage systems and marine environments, which are subjected to harsher environments. The environmental degradation mechanism mainly encompasses two categories: Type I and Type II hot corrosion^[53]. Type I corrosion occurs above 800–900 °C and can damage the protective oxide scale.

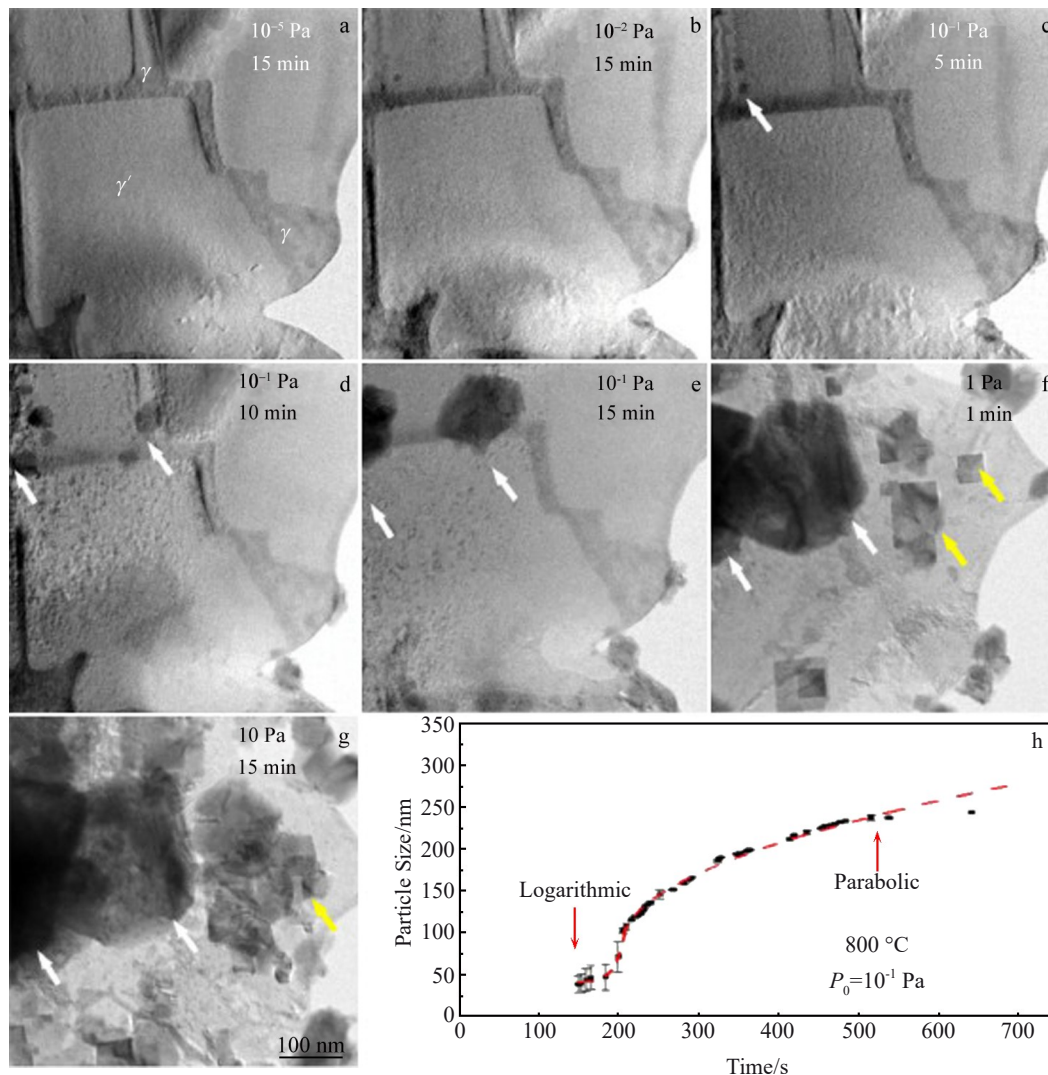


Fig.7 Typical TEM images of the oxidation process at a constant temperature of 800 °C under various oxygen pressures from 10^{-5} Pa to 10 Pa (a–g); particle size vs time at 800 °C under oxygen pressure of 10^{-1} Pa (red line represents the fitted curve) (h)^[51]

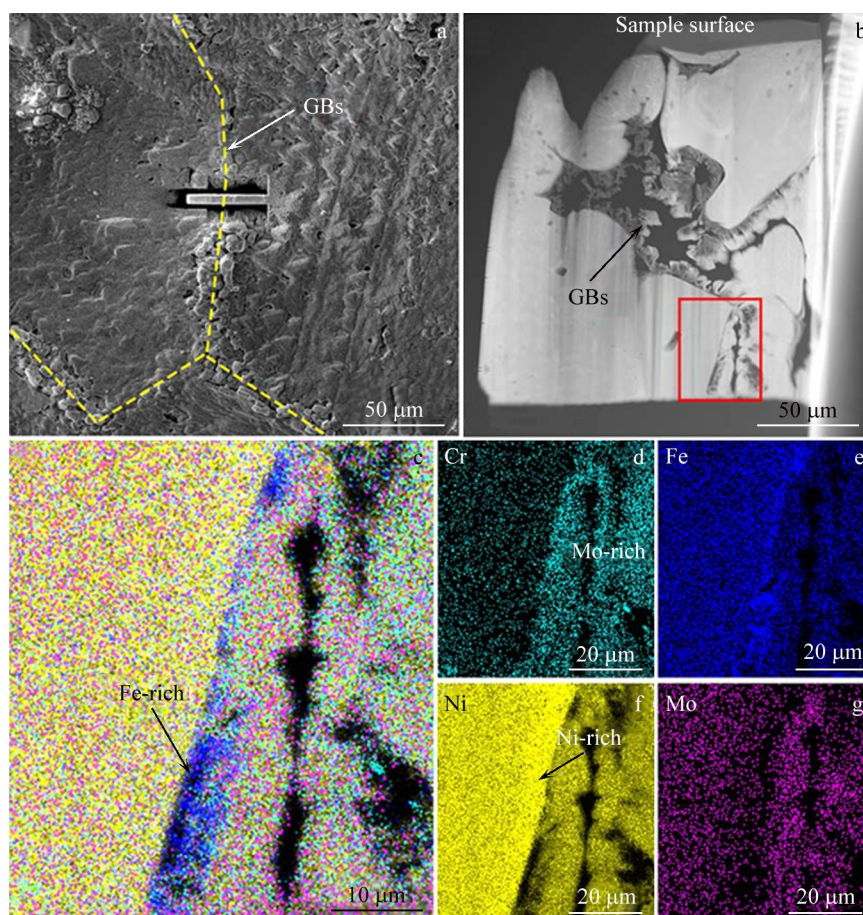


Fig.8 TEM analyses of the corrosion products of Hastelloy N exposed to FLiNaK molten salt environment: (a) FIB sampling position, (b) TEM image, (c) TEM image of red rectangle region in Fig.8b; corresponding EDS mappings of elements Cr (d), Fe (e), Ni (f), and Mo (g)^[9]

Type II corrosion tends to interact with the metal matrix to form liquid salt phases at 560–700 °C^[16]. Wang et al^[54] proved the hot corrosion behavior of a novel Ni16Cr13Co4Mo alloy in molten NaCl-KCl and NaCl-KCl-Na₂SO₄ through electrochemical measurements. The results show that the corrosion process is mainly governed by the diffusion of Cl₂ and SO₄²⁻. Elevated temperatures and the presence of Na₂SO₄ accelerate the corrosion rate. In molten NaCl-KCl salt, Cr₂O₃ dominates the corrosion products and exhibits p-type semiconductive properties. In molten NaCl-KCl-Na₂SO₄, intergranular corrosion appears, resulting in a corrosion layer that consists of an outer Cr₂O₃ layer (p-type) and an inner TiO₂-Al₂O₃ layer (n-type). Pradhan et al^[55] conducted research on the hot corrosion behavior of the superalloy IN718 in pure NaCl (salt S), salt mixtures of 60wt% Na₂SO₄+40wt% V₂O₅ (SM₁) and 75wt% Na₂SO₄+15wt% NaCl+10wt% V₂O₅ (SM₂) at 700 °C. The SM₁ samples suffer from severe corrosion due to the formation of highly corrosive NaVO₃, which significantly activates oxygen. Liu et al^[56] explored the hot corrosion behavior of a powder metallurgy-prepared superalloy under gas chloride salt-containing environment at 700, 750 and 800 °C. The results reveal that the penetration of chloride salts leads to the formation of cavities and cracks in the corrosion products, which deteriorate the oxide scales and accelerate the

oxidation rate. After oxidation for 100 h, the corrosion products include Cr₂O₃, TiO₂, Al₂O₃, NiO and NiCr₂O₄. Ma et al^[57] investigated the corrosion behavior of as-cast GH3625 alloy in different corrosive media (air, 75wt% Na₂SO₄+25wt% NaCl and 2% SO₂+H₂O+Air) at 900 °C for 120 h. The results reveal that the oxide film readily reacts with Cl⁻ to form gas Cl₂ and reacts with Na₂O to form Na₂CrO₄ when oxidized in molten salts medium, thereby causing the most severe corrosion. While in acid atmosphere, the continuous sulfurization and oxidation reactions of Cr and Ni with SO₂ and O₂ dominate the corrosion mechanism.

3 Summary and Prospects

Ni-based superalloys are vital materials used in aircraft engines, gas turbines, energy production, storage systems and chemical industries. It is imperative to further elevate the high-temperature oxidation resistance, mechanical properties, durability, and reliability of superalloys to withstand the harsh corrosive environment. We reviewed the recent progress of the effects of alloying elements and service environments on the oxidation resistance of Ni-based superalloys. Aluminum and chromium are beneficial elements that can form stable, compact and adhesive scales to protect the matrix from further oxidation. Recent researches have demonstrated that an

appropriate amount of silicon can facilitate the formation of Al_2O_3 or Cr_2O_3 - Al_2O_3 dual layer, which acts as an effective barrier against oxidation. Furthermore, silicon might restrain the internal penetration of sulfur. The p-type Ti-doping can promote the growth of Cr_2O_3 scale. Cobalt is an ideal element that can significantly enhance both the mechanical properties and corrosion resistance of materials. Molybdenum and tungsten elements were once considered to be detrimental in past decades, while recent researches reveal that a specific combination of these elements can actually stimulate the formation of Cr_2O_3 . Despite its reputation for exacerbating internal oxidation, it has been found that niobium can prevent the vaporization and spallation of Cr_2O_3 in external oxides when added in small quantities. An increase in tantalum content beyond 5wt% has been shown to enhance the high-temperature resistance of Ni-based superalloys. Hafnium addition is beneficial for optimizing the adhesion of oxide scales to the matrix at high temperatures.

The existence of hydrogen, sulfur, steam and high oxygen content in the atmosphere can accelerate the rapid oxidation of superalloy components. The oxidation mechanism of superalloys under various atmospheric conditions is thoroughly discussed. Oxidation temperature plays a critical role in the element diffusion behavior and oxide species, i.e., higher temperatures generally lead to an increase in oxide species, thereby enhancing the potential for spallation and accelerating the oxidation rate. Pressure may alter the initial nucleation sites of oxides, while stress can influence the elemental diffusion. However, it remains a subject of debate and further study whether these effects are positive or negative. Highly corrosive products tend to form in molten salt environments, which can deteriorate the alloy and accelerate the corrosion rate.

It is challenging to discern the influence of individual alloying elements on the microstructure, mechanical properties and oxidation resistance of superalloys due to the addition of more than eight alloying elements. The observed microstructure and properties are the result of synergistic effects of various alloying elements and complex factors of the surrounding environment. More efficient, accurate and specific methods should be developed to contribute to the investigation and improvement of superalloys. Numerous research endeavors have been undertaken to model the complex interactions during alumina formation, yet these models suffer from a paucity of reliable thermodynamic and kinetic databases for the concurrent formation of other oxides^[11,58]. Enhancing the predictive accuracy of these models remains a critical objective for future research. Traditional material development and optimization processes rely heavily on extensive experimental procedures, which are time-consuming and costly, and often fall short in meeting the intricate demands of superalloy fabrication. The rapid progress in high-performance computing and high-throughput computational screening has significantly expedited the exploration of superalloys and high entropy alloys. Density functional theory has gained widespread application in

calculating the microstructure and mechanical properties of materials^[59]. With the progression of the materials genome initiative, there is an urgent need to efficiently evaluate, analyze, manage and utilize big data to uncover fundamental material behavior patterns^[60]. Machine learning has emerged as a powerful tool for facilitating high-throughput screening of advanced materials with exceptional performance^[61-62]. Though these computational methods have accelerated the pace of material innovation, it is still hard to effectively fabricate superalloys with desired properties, since the vast uncharted territory and the whopping computational expenses present significant challenges in the effective fabrication of superalloys with desired attributes.

References

- 1 Ye Xianjue, Yang Biaobiao, Lai Ruilin et al. *Corrosion Science*[J], 2022, 198: 110100
- 2 Baik Sung-II, Yin Xin, Seidman David N. *Scripta Materialia*[J], 2013, 68(11): 909
- 3 Gao Shuang, He Bo, Zhou Lanzhang et al. *Corrosion Science*[J], 2020, 170: 108682
- 4 Wollgarten K, Galiullin T, Nowak W J et al. *Corrosion Science*[J], 2020, 173: 108774
- 5 Li Tiepan. *High Temperature Oxidation and Thermal Corrosion of Metals*[M]. Beijing: Chemical Industry Press Co., Ltd, 2003 (in Chinese)
- 6 Volders Cameron, Angelici Valentina Avincola, Waluyo Iradwikanari et al. *npj Materials Degradation*[J], 2022, 6(1): 52
- 7 Takakuwa Osamu, Ogawa Yuhei, Miyata Ryunosuke. *Scientific Reports*[J], 2023, 13(1): 6804
- 8 Li Meng, Wang Ping, Yang Yanqiu et al. *Journal of Materials Science*[J], 2022, 57(5): 3822
- 9 Gu Yufen, Zhang Wenzhu, Xu Youwei et al. *npj Materials Degradation*[J], 2022, 6(1): 90
- 10 Dai Jingjie, Sun Caixia, Wang Amin et al. *Corrosion Science*[J], 2021, 184: 109336
- 11 Sun Xiaoyu, Zhang Longfei, Pan Yanming et al. *Corrosion Science*[J], 2020, 162: 108216
- 12 Wise G J, Mignanelli P M, Hardy M C et al. *High Temperature Corrosion of Materials*[J], 2023, 99(3): 241
- 13 Wang Erpeng, Sun Duanjun, Liu Haifei et al. *Oxidation of Metals*[J], 2019, 92(3): 151
- 14 Anzini E, Glaenger N, Mignanelli P M et al. *Corrosion Science*[J], 2020, 176: 109042
- 15 Cockings H L, Perkins K M, Dowd M. *Materials Science and Technology*[J], 2017, 33(9): 1048
- 16 Barth T L, Marquis E A. *Oxidation of Metals*[J], 2019, 92(1): 13
- 17 Pan Qinghai, Zhao Xinbao, Yue Quanzhao et al. *Journal of Materials Research and Technology*[J], 2022, 20: 3074
- 18 Caldwell E C, Fela F J, Fuchs G E. *JOM*[J], 2004, 56(9): 44
- 19 Bopape Itshepeng Mogaleadi Christinah, Ogunmuyiwa Enoch

- Nifise, Shongwe Mxolisi Brendon et al. *International Journal of Advanced Manufacturing Technology*[J], 2022, 119(1): 287
- 20 Lu Jintao, Huang Jinyang, Yang Zhen et al. *Oxidation of Metals*[J], 2018, 89(1): 197
- 21 Meng Junsheng, Chen Mingxuan, Shi Xiaoping et al. *Transactions of Nonferrous Metals Society of China*[J], 2021, 31(8): 2402
- 22 Darolia R. *International Materials Reviews*[J], 2019, 64(6): 355
- 23 Lutton C K, Demarest C R, Gerard A Y et al. *Current Opinion in Solid State and Materials Science*[J], 2019, 23(3): 129
- 24 Ye Xianjue, Yang Biaobiao, Nie Yan et al. *Corrosion Science*[J], 2021, 185: 109436
- 25 Park Si Jun, Seo Seong Moon, Yoo Young Soo et al. *Corrosion Science*[J], 2015, 90: 305
- 26 Guo Hongbo, Wang Di, Peng Hui et al. *Corrosion Science*[J], 2014, 78: 369
- 27 Han F F, Chang J X, Li H et al. *Journal of Alloys and Compounds*[J], 2015, 619: 102
- 28 Yang Zhikun, Wang Hao, Zhang Yiwen et al. *Rare Metal Materials and Engineering*[J], 2021, 50(9): 3233
- 29 Taylor C D, Tossey B M. *npj Materials Degradation*[J], 2021, 5(1): 38
- 30 Hou J S, Guo J T, Wu Y X et al. *Materials Science and Engineering A*[J], 2010, 527(6): 1548
- 31 Rehman Khalil, Sheng Naicheng, Fan Shigang et al. *Acta Metallurgica Sinica (English Letters)*[J], 2022, 35(10): 1744
- 32 Yun Dae Won, Seo S M, Jeong H W et al. *Corrosion Science*[J], 2014, 83: 176
- 33 Pedrazzini S, Child D J, West G et al. *Scripta Materialia*[J], 2016, 113: 51
- 34 Li Xiaoli, He Shangming, Liang Jianping et al. *Oxidation of Metals*[J], 2019, 92(1): 67
- 35 Guo Hongbo, Li Dongqing, Zheng Lei et al. *Corrosion Science*[J], 2014, 88: 197
- 36 Xu Wenliang, Wang Fu, Ma Dexin et al. *Journal of Alloys and Compounds*[J], 2020, 17: 153337
- 37 Thanneeru R, Patil S, Deshpande S et al. *Acta Materialia*[J], 2007, 55(10): 3457
- 38 Rehman Khalil, Sheng Naicheng, Sang Zhiru et al. *Vacuum*[J], 2021, 191: 110382
- 39 Liu Longfei, Wu Shusen, Chen Yang et al. *Transactions of Nonferrous Metals Society of China*[J], 2016, 26(4): 1163
- 40 Ogawa Yuhei, Noguchi Kohei, Takakuwa Osamu. *Acta Materialia*[J], 2022, 229: 117789
- 41 Takakuwa Osamu, Ogawa Yuhei, Yamabe Junichiro et al. *Materials Science and Engineering A*[J], 2019, 739: 335
- 42 Liu Chang, Feng Haomin, Yang Yikai et al. *Intermetallics*[J], 2022, 142: 107446
- 43 Allo Justine, Jouen Samuel, Roussel Manuel et al. *Oxidation of Metals*[J], 2021, 95(5): 359
- 44 Kai W, Cheng F P, Chien F C et al. *Corrosion Science*[J], 2019, 158: 108093
- 45 Archana M, Rao C J, Ningshen S et al. *Journal of Materials Engineering and Performance*[J], 2021, 30(2): 931
- 46 Wu Ying, Narita Toshio. *Surface and Coatings Technology*[J], 2007, 202(1): 140
- 47 Xiao Jiuhuan, Xiong Ying, Wang Li et al. *International Journal of Minerals, Metallurgy and Materials*[J], 2021, 28(12): 1957
- 48 Wang Jue, Xue Hao, Wang Ying. *Rare Metals*[J], 2021, 40(3): 616
- 49 Cao Jiangdong, Jiang Bochen, Cao Xueyu et al. *Rare Metal Materials and Engineering*[J], 2021, 50(12): 4288
- 50 Li Dongsheng, Chen Guang, Li Dan et al. *Rare Metals*[J], 2021, 40(11): 3235
- 51 Zhai Yadi, Chen Yanhui, Zhao Yunsong et al. *Acta Materialia*[J], 2021, 215: 116991
- 52 Ramsay J D, Evans H E, Child D J et al. *Corrosion Science*[J], 2019, 154: 277
- 53 Rapp Robert A. *Corrosion Science*[J], 2002, 44(2): 209
- 54 Wang J H, Li D G, Shao T M. *Corrosion Science*[J], 2022, 200: 110247
- 55 Pradhan Dhananjay, Mahobia Girija Shankar, Chattopadhyay Kausik et al. *Journal of Materials Engineering and Performance*[J], 2018, 27(8): 4235
- 56 Liu Delin, Yang Wenhui, Chen Yang et al. *Oxidation of Metals*[J], 2022, 98(3): 325
- 57 Ma Yuanjun, Ding Yutain, Liu Jianjun et al. *Rare Metal Materials and Engineering*[J], 2022, 51(5): 1713
- 58 Sato A, Chiu Y L, Reed R C. *Acta Materialia*[J], 2011, 59(1): 225
- 59 Aykol M, Kim S, Hegde V I et al. *Nature Communications*[J], 2016, 7(1): 113779
- 60 Chen An, Zhang Xu, Zhou Zhen. *InfoMat*[J], 2020, 2(3): 553
- 61 Lu Shuaihua, Zhou Qionghua, Guo Yilv et al. *Advanced Materials*[J], 2020, 32(29): 2002658
- 62 Liu Fangning, Wang Yue, Ruixia Sun. *Materials China*[J], 2022, 41(11): 938 (in Chinese)

成分及环境对镍基高温合金氧化行为的影响

陈 阳, 胡凯翀, 黄海亮

(烟台大学 精准材料高等研究院, 山东 烟台 264005)

摘 要: 镍基高温合金在恶劣环境下具有优异的力学性能和耐高温性能。镍基高温合金的氧化行为高度依赖于材料的固有性能和氧化膜性能, 而氧化膜性能主要取决于合金元素的种类和含量。大气成分、温度、应力、熔融盐等各种环境参数是直接影响材料氧化行为的基本因素。综述了合金元素和服役环境对镍基高温合金氧化行为的影响。铝、铬和钴是有利元素, 可以形成致密、结合力强的氧化膜, 以保护基体。钛、钼、铌、钨、钽的添加一般被认为会削弱抗氧化性能, 但最近的研究有不同的观点。讨论了镍基高温合金的氧化机理, 并对镍基高温合金的未来发展进行了展望。

关键词: 氧化行为; 镍基; 高温合金; 合金元素; 服役环境

作者简介: 陈 阳, 女, 1993年生, 博士, 实验师, 烟台大学精准材料高等研究院, 山东 烟台 264005, E-mail: chen yang@ytu.edu.cn